Inorganic Chemistry

Article

pubs.acs.org/IC

Thermoelectric Properties of the Quaternary Chalcogenides $BaCu_{5.9}STe_6$ and $BaCu_{5.9}SeTe_6$

Mohamed Oudah, Katja M. Kleinke, and Holger Kleinke*

Department of Chemistry and Waterloo Institute for Nanotechnology, University of Waterloo, Waterloo, Ontario N2L 3G1, Canada

Supporting Information

ABSTRACT: These quaternary chalcogenides are isostructural, crystallizing in a unique structure type comprising localized Cu clusters and Te_2^{2-} dumbbells. With less than six Cu atoms per formula unit, these materials are p-type narrow-gap semiconductors, according to the balanced formula $Ba^{2+}(Cu^{+})_6Q^{2-}(Te_2^{2-})_3$ with Q = S, Se. Encouraged by the outstanding thermoelectric performance of $Cu_{2-x}Se$ and the low thermal conductivity of cold-pressed $BaCu_{5.7}Se_{0.6}Te_{6.4}$, we determined the thermoelectric properties of hot-pressed pellets of $BaCu_{5.9}STe_6$ and $BaCu_{5.9}SeTe_6$. Both materials exhibit a high Seebeck coefficient and a low electrical conductivity, combined with very low thermal conductivity below 1 W m^{-1} K^{-1}. Compared to the sulfide–telluride, the selenide–telluride exhibits higher electrical and thermal conductivity and comparable Seebeck coefficient, resulting in superior figure-of-merit values zT, exceeding 0.8 at relatively low temperatures, namely, around 600 K.

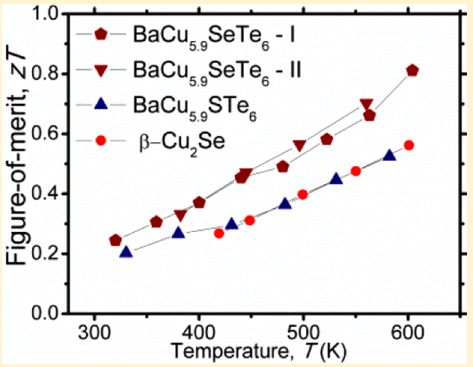

INTRODUCTION

Thermoelectric materials can convert waste heat into electricity and are thus of increasing importance in today's society, given the growing need for alternative energy sources. Many advanced thermoelectric materials are based on narrow-gap semiconductors formed by heavily doped heavy-metal chalcogenides including thallium, bismuth, and lead tellurides.[1−6] The heavy-metal atoms from the sixth period, Tl, Bi, and Pb, contribute to low thermal conductivity, κ, an important criterion for thermoelectrics: increasing thermoelectric figure of merit, zT, occurs with increasing efficiency, and zT is inversely proportional to κ. Other important criteria are a high Seebeck coefficient, α, and a high electrical conductivity, σ, according to the definition of $zT = T\alpha^2\sigma\kappa^{-1}$ (with T = absolute temperature).

Another way to achieve low thermal conductivity may lie in the cation mobility, such as mobile Cu ions. This was demonstrated in the case of $Cu_{2-x}Se$, which exhibits very low thermal conductivity, culminating in a high zT value of 1.5 at 1000 K.[7] The Cu-ion conductivity, on the other hand, causes well-documented stability issues, inhibiting the use of this material in actual thermoelectric devices, as the ions move with the temperature gradient.[8] We have been investigating new barium–copper chalcogenides for several years, aiming to find materials with localized Cu-ion conductivity, where the sixth-period Ba ions would impede the Cu paths as well as contribute to low thermal conductivity. This research led to the discovery of several new p-type semiconducting materials, including $Ba_3Cu_{14-x}Te_{12}$,[9] $Ba_{6.76}Cu_{2.42}Te_{14}$,[10] $Ba_2Cu_{4-x}Te_5$ and $Ba_2Cu_{4-x}Se_yTe_{5-y}$,[11] $Ba_2Cu_{6-x}STe_4$ and $Ba_2Cu_{6-x}Se_yTe_{5-y}$,[12] $BaCu_{6-x}STe_6$ and $BaCu_{6-x}Se_{1-y}Te_{6+y}$,[13] and $Ba_3Cu_{17-x}Se_{11-y}Te_y$.[14] One- and three-dimensional metallic properties were found in $Ba_2Cu_{7-x}Te_6$[15] and $Ba_3Cu_{17-x}S_{11.5-y}Te_y$,[16] respectively. All of these materials exhibit Cu clusters (with Cu–Cu bonds) as well as Cu atom deficiencies (hence, the p-type character).[17] In most cases, the Cu atom network is infinite in at least one direction, possibly leading to infinite diffusion paths of the Cu atoms. Notable exceptions are $Ba_{6.76}Cu_{2.42}Te_{14}$, $BaCu_{6-x}STe_6$, and $BaCu_{6-x}Se_{1-y}Te_{6+y}$, with the former exhibiting very low electrical conductivity because of its high Ba content. With this contribution, we present the thermoelectric properties of $BaCu_{6-x}STe_6$ and $BaCu_{6-x}Se_{1-y}Te_{6+y}$.

EXPERIMENTAL SECTION

Syntheses and Analyses. The title compounds were synthesized from the constituent elements stored in an argon-filled glovebox (Ba pieces, 99.7%, Strem Chemicals; Cu powder, 99.5%, Alfa Aesar; S flakes, 99.98%, Aldrich; Se pellets, 99.9%, Alfa Aesar; Te broken ingots, 99.99%, Strem Chemicals). The surface of the Ba pieces was scraped off to reduce contamination with O. Three samples were prepared, namely, one $BaCu_{5.9}STe_6$ and two $BaCu_{5.9}SeTe_6$ samples, because according to our earlier experiments we can only obtain phase-pure samples with 5.9 Cu atoms per formula unit. The elements were loaded in the desired stoichiometric 1:5.9:1:6 ratios into C-coated silica tubes, which were then evacuated up to ~10^{-3} mbar. The silica tubes were then sealed with a H_2/O_2 flame and then placed in a programmable resistance furnace for heat treatment. The furnace was programmed to reach 773 K within 24 h, followed by cooling to 673 K over 200 h and finally to room temperature by turning off the heat. Cooling slowly through the 773–673 K range led to incomplete

Special Issue: To Honor the Memory of Prof. John D. Corbett

Received: August 22, 2014
Published: October 9, 2014

ACS Publications © 2014 American Chemical Society

crystallization of the target materials because the melting point of $BaCu_{5.9}SeTe_6$ is incongruent at 718 K, as determined by differential scanning calorimetry measurement.[13] Thus, these samples were ground and then annealed at 663 K for 240 h to achieve homogeneity. After the annealing step, the samples were phase-pure according to their powder patterns obtained from the ground samples on an Inel powder diffractometer, which was equipped with a position-sensitive detector and utilized Cu $K\alpha_1$ radiation.

The three pure samples were hot-pressed into round disk pellets with a diameter of 12.7 mm and a thickness of ~2 mm under a flow of argon in a graphite die using the FR-210-30T hot press (Oxy-Gon Industries). The optimized pressing conditions for the Se-containing compound were 47 MPa at 628 K for 1.5 h, while the S-containing compound required slightly higher pressure and temperature, namely, 54 MPa and 653 K, to reach a comparable density. The densities for the pressed pellets were determined via the Archimedes method, which yielded >97% of the theoretical maximal values in all cases presented here.

The purities after the property measurements were confirmed via powder X-ray diffraction as well. No changes were found in the patterns after hot-pressing and after the final property measurements, indicative of the sufficient stability of these chalcogenides under those conditions. With the exception of a few minor highlighted peaks (open circles in Figure 1), all identified peaks belonged to the target compound.

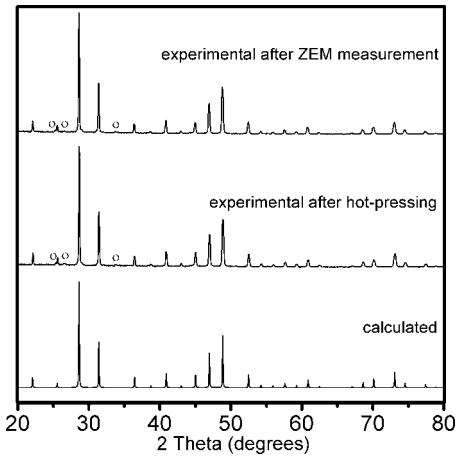

Figure 1. Experimental (top and center) and calculated (bottom) powder diagrams of $BaCu_{5.9}SeTe_6$.

Energy-dispersive X-ray spectroscopy (EDX) was performed on selected spots of the pellet surfaces of the S and first Se sample using a Zeiss Ultra scanning electron microscope and *EDAX Team* software. The acceleration voltage was 25 kV under high dynamic vacuum, and the ratios of elements were determined from the observed spectrum. The ratios of the elements were homogeneous in both samples and reasonably close to the expected values. The Ba:Cu:Se:Te ratio for the first Se-containing sample was 8.3:41.6:5.1:45.0 in atom %, while the Ba:Cu:S:Te ratio for the S-containing sample was 8.5:43.5:7.5:40.5. Both compare reasonably well to the expected atom % of 7.2:42.4:7.2:43.2, considering that concentrations below 10% are difficult to quantify with this method. No impurities from the reaction container or atmosphere (C, Si, or O) were detected. EDX mapping, which shows the elemental distribution across the scanned area of the sample with different colors assigned to different elements, was done on a Se-containing pellet to confirm homogeneity (Figure 2), with the top right part (labeled SEI) displaying the secondary electron image.

Physical Property Measurements. The pellets produced via hot-pressing were polished using 1000-grit sandpaper and spray-coated with C in preparation for the thermal diffusivity, λ, measurements using the Anter Flashline 3000 (now TA Instruments) under argon up to 620 K, which utilizes a flash method. The thermal conductivity, κ,

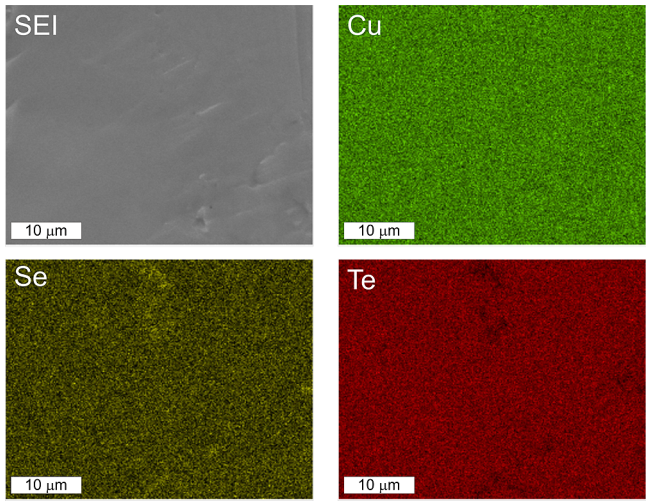

Figure 2. EDX maps of a $BaCu_{5.9}SeTe_6$ pellet. Top left: secondary electron image, SEI. Top right: Cu map. Bottom left: Se. Bottom right: Te.

was calculated via $\kappa = \rho\lambda C_P$, where ρ is the experimentally determined density, λ the measured diffusivity, and C_P the specific heat capacity estimated as the Dulong–Petit limit for each compound. The Dulong–Petit limit serves as a good approximation because of the lack of reliable experimental heat capacity data.[18]

For electrical-transport measurements, rectangular pellets, of approximately 10 × 2 × 2 mm, were cut out of the disks previously used. The Seebeck coefficient, α, and electrical conductivity, σ, were measured under helium as a function of the temperature up to 620 K by a four-probe method, using the ULVAC-RIKO ZEM-3.[19] The measurements were repeated on the same pellets to check for stability of both materials, $BaCu_{5.9}STe_6$ and $BaCu_{5.9}SeTe_6$, with the results being displayed in the Supporting Information, Figure S1. Finally, the materials were ground after the ZEM measurement and their X-ray patterns determined (see the Results and Discussion section and Figure 1).

RESULTS AND DISCUSSION

Crystal Structure. The unit cells of these isostructural polychalcogenides are surprisingly small, considering the complex formula containing four different elements, in particular in comparison with the other barium–copper chalcogenides.[17] Only one formula unit occurs per cubic unit cell, with a lattice parameter on the order of 6.9 Å. The Cu atoms, located on Wyckoff position 8i, form a cube centered around the S or Se atom located in the origin (1a). The Te atoms (6f) cap the edges of the Cu cubes and occur as Te_2^{2-} dumbbells. The Ba atom (1b) is placed in the center of the unit cell and is thus surrounded by a Cu_8Te_{12} pentagonal dodecahedron.

The Cu site is statistically occupied to 5.9/8 = 74% in $BaCu_{5.9}SeTe_6$; roughly two Cu atoms are missing per unit cell (or cube). With direct Cu–Cu contacts of 2.7–2.8 Å within the cube, the Cu atoms are likely locally mobile within each cube. The path from cube to cube, on the other hand, is obstructed by the Te and Ba atoms. This is demonstrated in Figure 3, wherein two Cu atoms per cube are shown in a lighter color to demonstrate possible positions of the vacancies. Therefore, the Cu atoms cannot move throughout the crystal and thus do not cause deterioration of the properties during cycling (as far as determined).

These materials would be intrinsic semiconductors with six Cu atoms per unit cell, according to the formula (Ba^{2+})-

dx.doi.org/10.1021/ic502055z | *Inorg. Chem.* 2015, 54, 845–849

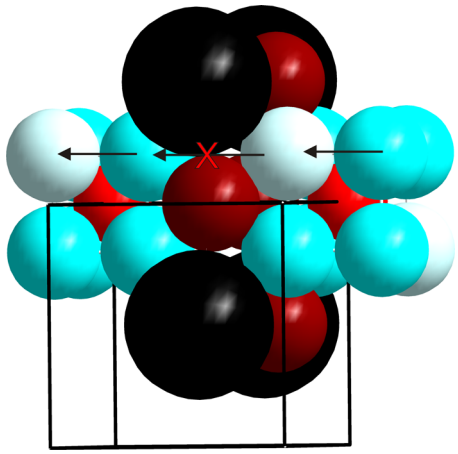

Figure 3. Part of the $BaCu_{5.9}SeTe_6$ unit cell: large black, Ba; blue, Cu; bright red, Se; dark red, Te; bright blue, Cu vacancies. The atoms are scaled according to their Slater radii.

$(Cu^+)_6Se^{2-}(Te_2^{2-})_3$, as confirmed via density functional theory calculations.[13] We have not been able to synthesize such a compound; the highest amount of Cu per cell experimentally obtained was 5.93(2). The material should be an extrinsic p-type semiconductor with 5.9 Cu atoms per cell, nominally with 3×10^{20} carriers cm^{-3} if no other defects were present.

Physical Properties. Two different samples of equivalent stoichiometry, called $BaCu_{5.9}SeTe_6$-I and $BaCu_{5.9}SeTe_6$-II, as well as one $BaCu_{5.9}STe_6$ sample were characterized. The electrical conductivity data are indicative of extrinsic semiconductors because the conductivity, σ, decreases at first with increasing temperature and then begins to increase once the intrinsic carriers have enough energy to cross the band gap. This turnaround in σ happens around 500 K in all three samples (Figure 4).

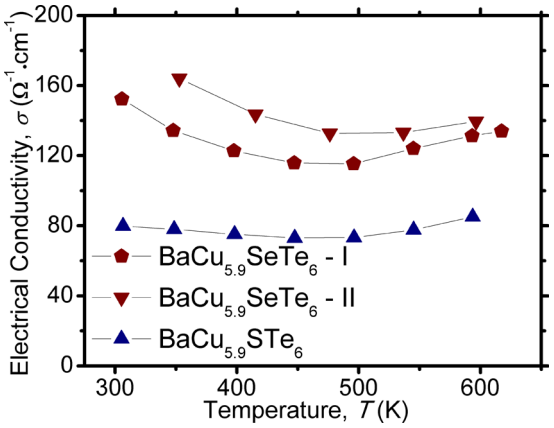

Figure 4. Electrical conductivity of $BaCu_{5.9}STe_6$ and $BaCu_{5.9}SeTe_6$.

The selenide sample II exhibits slightly larger σ values than sample I, while the sulfide exhibits much lower values, for example, 78 Ω^{-1} cm^{-1} compared to 133 Ω^{-1} cm^{-1} of selenide I and 164 Ω^{-1} cm^{-1} of selenide II around 350 K. With estimated experimental errors of 5%, the differences are significant. The lower conductivity of the sulfide may be a consequence of its more ionic character, which decreases the mobility. That the selenides are slightly different is likely a consequence of minor weighing errors, which impact the carrier concentration. These numbers, summarized in Table 1, are relatively low for

Table 1. Thermoelectric Properties of $BaCu_{5.9}STe_6$ and $BaCu_{5.9}SeTe_6$[a]

	$BaCu_{5.9}STe_6$	$BaCu_{5.9}SeTe_6$-I	$BaCu_{5.9}SeTe_6$-II
property	350 K/560 K	350 K/560 K	350 K/560 K
σ [Ω^{-1} cm^{-1}]	78/80	133/126	164/136
α [μV K^{-1}]	223/201	201/216	190/228
PF [μW cm^{-1} K^{-2}]	3.9/3.2	5.4/5.9	5.9/7.0
L [10^{-8} V^2 K^{-2}]	1.59/1.62	1.62/1.60	1.64/1.58
κ [W m^{-1} K^{-1}]	0.58/0.37	0.64/0.51	0.67/0.56
κ_L [W m^{-1} K^{-1}]	0.53/0.30	0.57/0.39	0.58/0.44
zT	0.24/0.49	0.30/0.65	0.31/0.70[b]

[a]The power factor was calculated via $PF = \alpha^2\sigma$. The Lorenz number, L, was calculated from the Seebeck coefficient, α, and used to derive the lattice thermal conductivity, κ_L, from the total thermal conductivity κ via $\kappa_L = \kappa - L\sigma T$. Finally, the figure of merit, zT, was calculated via $zT = T\alpha^2\sigma\kappa^{-1}$. [b]$zT$ exceeds 0.8 at 600 K.

advanced thermoelectric materials. For example, β-Cu_2Se shows σ = 540 Ω^{-1} cm^{-1} at 420 K and continuously decreases throughout the analyzed temperature range, down to 320 Ω^{-1} cm^{-1} at 600 K and 130 Ω^{-1} cm^{-1} at 1000 K.[7]

The temperature dependence of the Seebeck coefficient, α, is presented in Figure 5. All curves are rather flat, with

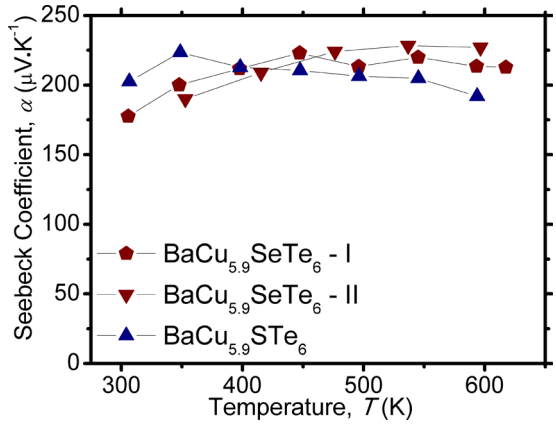

Figure 5. Seebeck coefficient of $BaCu_{5.9}STe_6$ and $BaCu_{5.9}SeTe_6$.

comparable α values on the order of 175−230 μV K^{-1}. Some of these values are equivalent within the estimated experimental error of 3%. For comparison, α increases steadily in the case of β-Cu_2Se from 110 μV K^{-1} at 420 K to 170 μV K^{-1} at 600 K and 300 μV K^{-1} at 1000 K.[7] In the case of a clear maximum, as found in the sulfide, one can use the band gap, E_{gap}, approximation popularized by Goldsmid from the maximum α and the corresponding temperature via $E_{gap} = 2e\alpha_{max}T_{max}$, with e = electron charge.[20] Using α_{max} = 223 μV K^{-1} and T_{max} = 349 K, we calculate E_{gap} = 0.16 eV for the sulfide. With α_{max} = 223 μV K^{-1} and T_{max} = 447 K, one obtains E_{gap} = 0.20 eV for selenide I, and with 228 μV K^{-1} and 447 K, E_{gap} = 0.24 eV (selenide II). Because of the broad maxima in the case of the selenides, these values are less reliable but are in the same range as the sulfide and in line with the results of the electronic structure calculations.

The nominator of the thermoelectric figure of merit, the power factor, $PF = \alpha^2\sigma$, serves as a measure of the electrical performance of thermoelectric materials. As depicted in Figure 6, PF decreases above 350 K in the case of the sulfide, with values from 3.9 to 3.1 μW cm^{-1} K^{-1} at 590 K, whereas PF

dx.doi.org/10.1021/ic502055z | Inorg. Chem. 2015, 54, 845−849

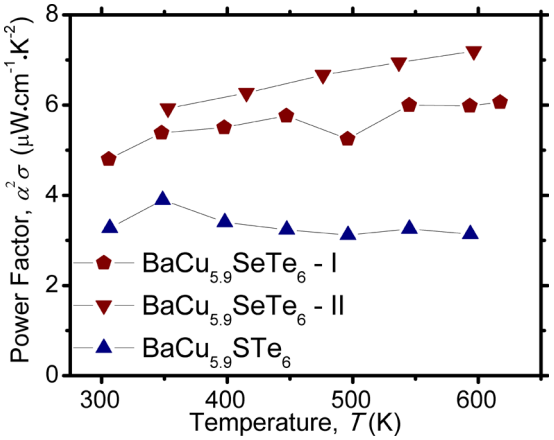

Figure 6. PF of $BaCu_{5.9}STe_6$ and $BaCu_{5.9}SeTe_6$.

generally increases with increasing temperature in the case of the selenide, e.g., from 4.8 μW cm^{-1} K^{-1} at 300 K up to 6.1 μW cm^{-1} K^{-1} at 617 K. The latter trend is also present in β-Cu_2Se, with PF increasing from 6.7 μW cm^{-1} K^{-1} at 420 K to 9.2 μW cm^{-1} K^{-1} at 600 K (and 11.5 μW cm^{-1} K^{-1} at 1000 K).[7] Thus, the electrical performance of β-Cu_2Se is superior compared to $BaCu_{5.9}SeTe_6$, with the sulfide being a distant third.

The thermal conductivity, κ, data of the title compounds are presented in Figure 7. Overall, the values are very low,

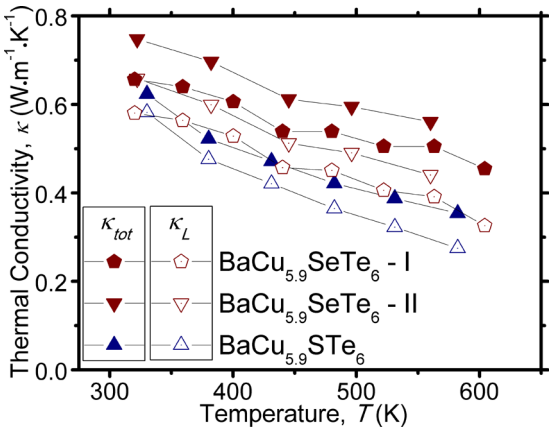

Figure 7. Thermal conductivity of $BaCu_{5.9}STe_6$ and $BaCu_{5.9}SeTe_6$. Filled symbols: total thermal conductivity, κ_{tot}. Open symbols: lattice thermal conductivity, κ_L.

consistently below 0.8 W m^{-1} K^{-1}, which is even lower than that for β-Cu_2Se (1.04 W m^{-1} K^{-1} at 420 K and 0.98 W m^{-1} K^{-1} at 600 K).[7] All values decrease with increasing temperature because of the increase in phonon−phonon scattering, with the sulfide exhibiting the lowest values, running from 0.62 W m^{-1} K^{-1} at 330 K to 0.35 W m^{-1} K^{-1} at 580 K, and the selenide II exhibiting the highest values, namely, from 0.75 W m^{-1} K^{-1} at 320 K to 0.56 W m^{-1} K^{-1} at 560 K. Even with an estimated error of 5%, the selenide I still has slightly lower values, e.g., 0.66 W m^{-1} K^{-1} ($\pm$0.03 W m^{-1} K^{-1}) at 320 K.

To analyze whether or not the differences in κ are simply a consequence of the different carrier concentrations, we utilized the Wiedemann−Franz law to estimate the electronic contribution $\kappa_{el} = L\sigma T$ to the total thermal conductivity. The Lorenz number, L, depends on the material and the temperature and is typically between 2.44 × 10^{-8} V^2 K^{-2} (Sommerfeld value; degenerate semiconductors) and 1.5 × 10^{-8} V^2 K^{-2} (intrinsic semiconductors).[21] We calculated L by utilizing the single parabolic band and elastic carrier scattering assumption from the experimental Seebeck coefficient as described before,[22] assuming acoustic phonon and/or alloying scattering (both resulting in the scattering parameter λ being 0).[23] Subtracting κ_{el} from the total thermal conductivity yields the lattice thermal conductivity, $\kappa_L = \kappa - \kappa_{el}$, presented as open symbols in Figure 7 and included along with the respective Lorenz numbers in Table 1.

While the differences between κ_L are smaller than the differences between κ, the trends remain the same. Therefore, we conclude that the sulfide indeed exhibits the lowest lattice thermal conductivity here, at least at elevated temperatures, likely a consequence of the larger mass fluctuations in this material. The two selenides exhibit lattice thermal conductivity values that remain equivalent within the estimated errors. In addition to the heavy atoms and the Cu mobility, the large amount of vacancies (two per formula unit and unit cell) is likely to contribute to this very low thermal conductivity as discussed for various copper−gallium tellurides[24] and $(In_2Te_3)_x(GeTe)_{3-3x}$ samples.[25] Comparable thermal conductivity (κ < 0.8 W m^{-1} K^{-1}) also occurs in some thallium tellurides, where the heavy Tl atoms along with their distorted environment are a major factor for the small κ values,[5,6,24,26] and in $Yb_{14}MnSb_{11}$ with its huge, low-symmetry unit cell.[27]

Finally, the thermoelectric figure of merit, zT, was computed from the thermal conductivity data and fits to the experimental PF data that encompass the temperature range of the κ measurements. The data are presented up to 600 K in Figure 8

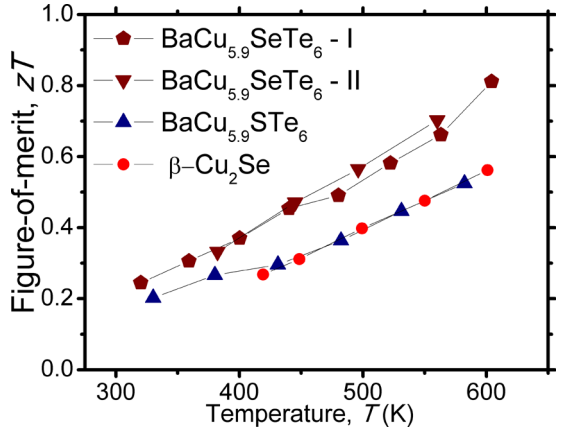

Figure 8. Thermoelectric figure of merit of $BaCu_{5.9}STe_6$ and $BaCu_{5.9}SeTe_6$ in comparison to β-Cu_2Se.

in comparison to β-Cu_2Se.[7] As is typical for doped semiconductors, the zT values increase with increasing temperature. The two selenide−telluride samples are the best thermoelectrics here, exhibiting basically equivalent values, ranging from zT = 0.23 at 320 K to 0.81 at 600 K. The sulfide−telluride falls behind, with zT values between 0.20 at 330 K and 0.52 at 580 K, precisely matching the performance of β-Cu_2Se in this temperature range.

CONCLUSIONS

The thermoelectric properties of the copper chalcogenides $BaCu_{5.9}STe_6$ and $BaCu_{5.9}SeTe_6$ were presented in comparison to β-Cu_2Se, one of the leading high-temperature thermo-

dx.doi.org/10.1021/ic502055z | Inorg. Chem. 2015, 54, 845−849

electrics. The best feature with regard to the thermoelectric properties is the extraordinarily low thermal conductivity, which, combined with low electrical conductivity and high Seebeck coefficient, results in outstanding thermoelectric figure of merit: the sulfide−telluride exhibits zT values comparable to that of β-Cu_2Se, while the selenide−telluride has superior properties within the investigated temperature range. On the plus side, the Ba-containing materials appear to not suffer from Cu-ion migration, which reflects itself in high stability; on the other hand, these materials decompose upon heating above 720 K.

On the basis of the relatively high Seebeck coefficient and low electrical conductivity, increasing the charge-carrier concentration via hole doping should result in higher zT values. Unfortunately, we were unable to produce more Cu-deficient samples. Therefore, we will attempt to raise the hole concentration (lower the electron concentration) via alternative routes in the future, e.g., via a partial substitution of Ba^{2+} with K^+, in order to verify this assumption.

■ ASSOCIATED CONTENT

Ⓢ Supporting Information

Graph displaying the figure of merit of repeat measurements on $BaCu_{5.9}STe_6$ and $BaCu_{5.9}SeTe_6$. This material is available free of charge via the Internet at http://pubs.acs.org.

■ AUTHOR INFORMATION

Corresponding Author

*E-mail: kleinke@uwaterloo.ca.

Notes

The authors declare no competing financial interest.

■ ACKNOWLEDGMENTS

Financial support from the Natural Sciences and Engineering Research Council is appreciated.

■ REFERENCES

(1) Rowe, D. M. *Thermoelectrics Handbook: Macro to Nano*; CRC Press, Taylor & Francis Group: Boca Raton, FL, 2006.
(2) Kleinke, H. *Chem. Mater.* **2010**, *22*, 604−611.
(3) Toberer, E. S.; May, A. F.; Snyder, G. J. *Chem. Mater.* **2010**, *22*, 624−634.
(4) Kanatzidis, M. G. *Chem. Mater.* **2010**, *22*, 648−659.
(5) Guo, Q.; Chan, M.; Kuropatwa, B. A.; Kleinke, H. *Chem. Mater.* **2013**, *25*, 4097−4104.
(6) Guo, Q.; Assoud, A.; Kleinke, H. *Adv. Energy Mater.* **2014**, *4*, 1400348/1-8.
(7) Liu, H.; Shi, X.; Xu, F.; Zhang, L.; Zhang, W.; Chen, L.; Li, Q.; Uher, C.; Day, T.; Snyder, G. J. *Nat. Mater.* **2012**, *11*, 422−425.
(8) Brown, D. R.; Day, T.; Caillat, T.; Snyder, G. J. *J. Electron. Mater.* **2013**, *42*, 2014−2019.
(9) Assoud, A.; Thomas, S.; Sutherland, B.; Zhang, H.; Tritt, T. M.; Kleinke, H. *Chem. Mater.* **2006**, *18*, 3866−3872.
(10) Cui, Y.; Assoud, A.; Xu, J.; Kleinke, H. *Inorg. Chem.* **2007**, *46*, 1215−1221.
(11) Mayasree, O.; Cui, Y. J.; Assoud, A.; Kleinke, H. *Inorg. Chem.* **2010**, *49*, 6518−6524.
(12) Mayasree, O.; Sankar, C. R.; Assoud, A.; Kleinke, H. *Inorg. Chem.* **2011**, *50*, 4580−4585.
(13) Mayasree, O.; Sankar, C. R.; Cui, Y.; Assoud, A.; Kleinke, H. *Eur. J. Inorg. Chem.* **2011**, 4037−4042.
(14) Kuropatwa, B.; Cui, Y.; Assoud, A.; Kleinke, H. *Chem. Mater.* **2009**, *21*, 88−93.
(15) Kuropatwa, B. A.; Assoud, A.; Kleinke, H. *Inorg. Chem.* **2012**, *51*, 5299−5304.
(16) Kuropatwa, B. A.; Assoud, A.; Kleinke, H. *Inorg. Chem.* **2011**, *50*, 7831−7837.
(17) Mayasree, O.; Sankar, C. R.; Kleinke, K. M.; Kleinke, H. *Coord. Chem. Rev.* **2012**, *256*, 1377−1383.
(18) Wang, H.; Porter, W. D.; Böttner, H.; König, J.; Chen, L.; Bai, S.; Tritt, T. M.; Mayolett, A.; Senawiratne, J.; Smith, C.; Harris, F.; Gilbert, P.; Sharp, J. W.; Lo, J.; Kleinke, H.; Kiss, L. I. *J. Electron. Mater.* **2013**, *42*, 1073−1084.
(19) Wang, H.; Porter, W. D.; Böttner, H.; König, J.; Chen, L.; Bai, S.; Tritt, T. M.; Mayolett, A.; Senawiratne, J.; Smith, C.; Harris, F.; Gilbert, P.; Sharp, J. W.; Lo, J.; Kleinke, H.; Kiss, L. I. *J. Electron. Mater.* **2013**, *42*, 654−664.
(20) Goldsmid, H. J.; Sharp, J. W. *J. Electron. Mater.* **1999**, *28*, 869−872.
(21) Kumar, G. S.; Prasad, G.; Pohl, R. O. *J. Mater. Sci.* **1993**, *28*, 4261−4272.
(22) Guo, Q.; Kleinke, H. *J. Solid State. Chem.* **2014**, *215*, 253−259.
(23) Cahill, D. G.; Watson, S. K.; Pohl, R. O. *Phys. Rev. B* **1992**, *46*, 6131−6140.
(24) Kurosaki, K.; Yamanaka, S. *Phys. Status Solidi* **2013**, *210*, 82−88.
(25) Sun, H.; Lu, X.; Chi, H.; Morelli, D. T.; Uher, C. *Phys. Chem. Chem. Phys.* **2014**, *16*, 15570−15575.
(26) Wölfing, B.; Kloc, C.; Teubner, J.; Bucher, E. *Phys. Rev. Lett.* **2001**, *86*, 4350−4353.
(27) Cox, C. A.; Toberer, E. S.; Levchenko, A. A.; Brown, S. R.; Snyder, G. J.; Navrotsky, A.; Kauzlarich, S. M. *Chem. Mater.* **2009**, *21*, 1354−1360.